Emittance Growth in Heavy Ion Rings Due to the Effects of Space Charge and Dispersion*

John J. Barnard, George D. Craig, Alex Friedman,
David P. Grote, Bojan Losic, and Steven M. Lund

Lawrence Livermore National Laboratory, L-645, Livermore, CA 94550

Abstract

We review the derivation of moment equations which include the effects of space charge and dispersion in bends first presented in ref. [1]. These equations generalize the familiar envelope equations to include the dispersive effects of bends. We review the application of these equations to the calculation of the change in emittance resulting from a sharp transition from a straight section to a bend section, using an energy conservation constraint. Comparisons of detailed 2D and 3D simulations of intense beams in rings using the WARP code (refs. [2,3]) are made with results obtained from the moment equations. We also compare the analysis carried out in ref. [1], to more recent analyses, refs. [4,5]. We further examine self-consistent distributions of beams in bends and discuss the relevance of these distributions to the moment equation formulation.

Introduction

There are many applications in which beams having non-negligible space charge forces are transported through bends. In heavy ion fusion (HIF), recirculating induction accelerators (recirculators), with large tune depressions, and with rapid acceleration through resonances, are being considered to ignite inertial confinement fusion targets. Even in linac approaches to HIF, designs of the final transport to the target usually include transport through 180 degrees or more of bend section. In some Acclerator Production of Tritium designs, a final bent transport section is being considered as part of an upgrade option. For the application of studying high energy density in matter, a beam pulse in a storage ring will be longitudinally compressed, reaching tune shifts for short periods much larger than allowed by the Laslett-tune shift limit. Even in traditional synchrotrons and storage rings obeying the Laslett limit, it is useful to have a framework in which space charge and dispersion are both included.

In the HIF application, the normalized emittance of the beam must remain small to be able to focus the beam on a small spot. The growth of the normalized emittance of an accelerated beam is also of interest for many other applications in which high brightness is required. The concept of transverse energy conservation was used in ref. [1] to study emittance growth in bends. This built upon earlier studies which have calculated changes in emittance also using a transverse energy constraint. For example, emittance growth associated with non-uniform space-charge distributions was examined in refs. [8]- [10]. Emittance growth due to initial beam displacements and mismatches with and without space-charge and momentum spread has been studied in, refs. [11-13,17], and references therein.

In the work reviewed here the beams propagate in continuous or alternating gradient focusing channel, with phase advances that are depressed due to space

* Work performed under the auspices of the U. S. Department of Energy by LLNL under contract W-7405-ENG-48.

CP448, *Workshop on Space Charge Physics in High Intensity Hadron Rings*
edited by A. U. Luccio and W. T. Weng

charge. In addition, bends are present, which provide a displacement in the center of oscillation for ions which are off of the design momentum. Moment equations are employed to estimate emittance growth arising from the transition from straight sections to bends. (See also ref. [14] for an estimate of emittance growth due to the transitions in the absence of space charge.) On a transition from a bend to a straight section, or from a straight section to a bend, if the transition is sufficiently sharp, the beam becomes mismatched. We assume that small nonlinear forces act to phase mix particles, and we find the asymptotic emittance of such a beam. Further, if we assume that the process of phase mixing is completed before the beam goes through another straight/bend transition, we may calculate the emittance growth through a "racetrack" configuration consisting of two 180° bends and two straight sections, even without a detailed knowledge of the rate at which the phase mixing occurs.

Model Equations of Motion

The force equation in the radial (bend) direction using cylindrical coordinates, (ρ, θ, y) is:

$$\ddot{\rho} - \frac{v_\theta^2}{\rho} = F_{bend} - v_\theta^2 k_{\beta 0x}^2(\rho - \rho_0) + v_\theta^2 k_{sx}^2(\rho - <\rho>) \tag{1}$$

Here, ρ is the radial coordinate of a particle in a bend, θ is the azimuthal coordinate, y is the vertical coordinate and $v_\theta \equiv \rho\dot{\theta}$ is the azimuthal velocity, and k_{sx}^2 is a defocusing constant of the assumed linear space charge force in the radial direction (defined below). For simplicity, non-relativistic kinematics are assumed. Also, ρ_0 is the nominal radius of a particle with the azimuthal component of the design momentum p_0 and design velocity $v_0 \equiv \beta c$.
The component of the bending force F_{bend} in the radial direction is given by:

$$F_{bend} = \left(\frac{qe}{Am_a}\right)\begin{cases} v_\theta B_y & \text{(magnetic bends)} \\ E_\rho & \text{(electric bends)} \end{cases} \tag{2}$$

Here q is the ion charge state (+1 for protons), e is the proton charge in Coulombs, A is the ion mass in amu, m_a is the atomic mass unit in kg. B_y is the vertical bending field (for magnetic bends) or E_ρ is the radial electric field (for electric bends).

We let $x \equiv \rho - \rho_0$ and define the increment in path length along the design orbit $ds \equiv \rho_0 d\theta$. The equations of motion are then given by,

$$x'' = -k_{\beta 0x}^2(x - x_m) + k_{sx}^2(x - x_c) - \frac{\partial h_{nl}(x,y)}{\partial x}. \tag{3}$$

$$y'' = -k_{\beta 0y}^2 y + k_{sy}^2(y - y_c) - \frac{\partial h_{nl}(x,y)}{\partial y}. \tag{4}$$

$$k_{sx}^2 \equiv \frac{K}{2(\Delta x^2 + (\Delta x^2 \Delta y^2)^{1/2})}; \qquad k_{sy}^2 \equiv \frac{K}{2(\Delta y^2 + (\Delta x^2 \Delta y^2)^{1/2})}. \tag{5}$$

Here, x is the in-plane deviation from the design orbit and y is the vertical coordinate in a particular transverse slice of the beam. The beam travels in the $+s$ direction, and prime ($'$) indicates derivative with respect to s; $k_{\beta 0x}$ and $k_{\beta 0y}$ can represent either alternating gradient focusing (if they are s dependent) or they can represent the focusing effects in the smooth approximation, in which case, $k_{\beta 0x} = k_{\beta 0y} = \sigma_0/2L$ where σ_0 is the undepressed phase advance, and L is the half-lattice period. Dispersion effects enter through the term x_m, where

$x_m \equiv (1/k_{\beta 0x}^2 \rho_0)(\delta p/p_0)$ for magnetic focusing and $x_m \equiv (2/k_{\beta 0x}^2 \rho_0)(\delta p/p_0)$ for electric focusing. The quantity $\delta p/p_0$ is the fractional difference between the longitudinal momentum of a particle and the design momentum p_0, and $K \equiv 2qI/(\beta^3 A I_o)$ is the perveance. Here $I_o \equiv 4\pi\epsilon_0 m_a c^3/e$ is the characteristic proton current ($\cong$31 MA). Finally, for generality, we have included an unspecified external non-linear potential h_{nl} that is a function of x,y, and possibly s.

We adopt the notation of ref. [1], throughout this paper in which the quantity Δ is reserved for the two argument operator in which centroid quantities are subtracted off: $\Delta ab \equiv < ab > - < a >< b >$ (e.g. $\Delta x^2 \equiv < x^2 > - < x >^2$), where $<>$ indicates average over all particles in a slice; $x_c \equiv < x >$, and $y_c \equiv < y >$.

These equations are identical to the equations found in ref. [1], except here we no longer assume $k_{\beta 0x}$, $k_{\beta 0y}$, and ρ_0 to be independent of s, nor do we require $k_{\beta 0x} = k_{\beta 0y}$. In deriving the moment equations in ref. [1], no use was made of the assumed constancy or equality of $k_{\beta 0x}$ and $k_{\beta 0y}$ nor the constancy of ρ_0, so the generalization simply amounts to a relabeling of the focusing constants.

Eqs. (3) and (4) represent, in an approximate way, the effects of: linear focusing, linear space charge defocusing, dispersion in a bend, and external non-linearities in the focusing field. The physical approximations that have been made include the following: (1) Eqs. (3) and (4) have been linearized in the small quantities $k_{\beta 0}x$, $k_{\beta 0}y$, and $\delta p/p_0$. (The non-linear term h_{nl} has also been included in some of the derivations). (2) The non-linearity is small: ($|h_{nl}| << |k_{\beta 0x}^2 x^2|, |k_{\beta 0y}^2 y^2|$). (Terms which are non-linear in $\delta p/p_0$, such as $k_{\beta 0} x \delta p/p_0$, have been neglected.) (3) Space charge forces depend only on lowest order moments. (We have used the KV formula for the electrostatic potential, which is equivalent to assuming uniform density elliptical beam. Centroid position and semi-major axes are, however, allowed to vary with s). (4) The beam is coasting: (p_0, β, and δp are constants). (5) The beam is non-relativistic: ($\beta << 1$).

Let $f(x, x', y, y', \frac{\delta p}{p_0}, s) = \mathrm{d}N/\mathrm{d}x\mathrm{d}x'\mathrm{d}y\mathrm{d}y'\mathrm{d}\frac{\delta p}{p_0}$ where $\mathrm{d}N$ is the number of particles within incremental phase volume $\mathrm{d}x\mathrm{d}x'\mathrm{d}y\mathrm{d}y'$ $\mathrm{d}\frac{\delta p}{p_0}$. For the model equations (3)-(5) the Vlasov equation becomes:

$$\frac{\partial f}{\partial s}+x'\frac{\partial f}{\partial x}+\left(-k_{\beta 0x}^2(x-x_m)+k_{sx}^2(x-x_c)-\frac{\partial h_{nl}}{\partial x}\right)\frac{\partial f}{\partial x'}+y'\frac{\partial f}{\partial y}+\left(-k_{\beta 0y}^2 y+k_{sy}^2(y-y_c)-\frac{\partial h_{nl}}{\partial y}\right)\frac{\partial f}{\partial y'} = 0. \tag{6}$$

The average of a variable ξ over the continuous distribution is given by:

$$< \xi > (s) \equiv \int \mathrm{d}x \int \mathrm{d}x' \int \mathrm{d}y \int \mathrm{d}y' \int \mathrm{d}\tfrac{\delta p}{p_0} \xi f(x, x', y, y', \tfrac{\delta p}{p_0}, s)/N,$$

where

$$N \equiv \int \mathrm{d}x \int \mathrm{d}x' \int \mathrm{d}y \int \mathrm{d}y' \int \mathrm{d}\tfrac{\delta p}{p_0} f(x, x', y, y', \tfrac{\delta p}{p_0}, s).$$

Following ref. [7], we take all second order moments of the Vlasov eq. (6), yielding eight (first-order with respect to s) coupled moment equations:

$$\begin{aligned}
&\tfrac{\mathrm{d}}{\mathrm{d}s}\Delta x^2 = 2\Delta x x' \\
&\tfrac{\mathrm{d}}{\mathrm{d}s}\Delta x'^2 = (-2k_{\beta 0x}^2 + 2k_{sx}^2)\Delta x x' + 2k_{\beta 0x}^2 \Delta x' x_m - 2\Delta(x' \tfrac{\partial h_{nl}}{\partial x}) \\
&\tfrac{\mathrm{d}}{\mathrm{d}s}\Delta x x' = \Delta x'^2 - k_{\beta 0x}^2 \Delta x^2 + k_{sx}^2 \Delta x^2 + k_{\beta 0x}^2 \Delta x x_m - \Delta(x \tfrac{\partial h_{nl}}{\partial x}) \\
&\tfrac{\mathrm{d}}{\mathrm{d}s}\Delta y^2 = 2\Delta y y' \\
&\tfrac{\mathrm{d}}{\mathrm{d}s}\Delta y'^2 = (-2k_{\beta 0y}^2 + 2k_{sy}^2)\Delta y y' - 2\Delta(y' \tfrac{\partial h_{nl}}{\partial y}) \\
&\tfrac{\mathrm{d}}{\mathrm{d}s}\Delta y y' = \Delta y'^2 - k_{\beta 0y}^2 \Delta y^2 + k_{sy}^2 \Delta y^2 - \Delta(y \tfrac{\partial h_{nl}}{\partial y}) \\
&\tfrac{\mathrm{d}}{\mathrm{d}s}\Delta x x_m = \Delta x' x_m \\
&\tfrac{\mathrm{d}}{\mathrm{d}s}\Delta x' x_m = -k_{\beta 0x}^2 \Delta x x_m + k_{sx}^2 \Delta x x_m + k_{\beta 0x}^2 \Delta x_m^2 - \Delta(x_m \tfrac{\partial h_{nl}}{\partial x})
\end{aligned} \tag{7}$$

Similarly, the first order moments of eq. (6) yield the following:

$$
\begin{aligned}
&\tfrac{\mathrm{d}}{\mathrm{d}s}x_c = x'_c\\
&\tfrac{\mathrm{d}}{\mathrm{d}s}x'_c = -k^2_{\beta 0x}x_c + k^2_{\beta 0x} < x_m > - < \tfrac{\partial h_{nl}}{\partial x} >\\
&\tfrac{\mathrm{d}}{\mathrm{d}s}y_c = y'_c\\
&\tfrac{\mathrm{d}}{\mathrm{d}s}y'_c = -k^2_{\beta 0y}y_c - < \tfrac{\partial h_{nl}}{\partial y} >
\end{aligned}
\tag{8}
$$

Note that if $h_{nl} = 0$, eq. (7) forms a closed sets of 8 equations, and eq. (8) forms two sets of two closed equations. If $h_{nl} \neq 0$, eqs. (7) and (8) form the beginning of an infinite hierarchy of moment equations.

Transverse Energy Conservation

For the case of alternating gradient focusing, and when the bends occupy only a fraction of the lattice, the focusing constants $k^2_{\beta 0x}$, $k^2_{\beta 0y}$, and the bend radius of curvature ρ_0 are dependent on s. This s-dependence of the external forces implies that there will not be a constant energy-like quantity. However, as in ref. [1], if $k_{\beta 0x}, k_{\beta 0y}$, and ρ_0 are constants representing average quantities, we may define a transverse energy H:

$$
\begin{aligned}
2H = {} & k^2_{\beta 0x}\Delta x^2 + k^2_{\beta 0y}\Delta y^2 + \Delta x'^2 + \Delta y'^2 - 2k^2_{\beta 0x}\Delta x x_m - K \ln\left((\Delta x^2)^{1/2} + (\Delta y^2)^{1/2}\right)\\
& +2 < h_{nl} > + k^2_{\beta 0x}x_c^2 + k^2_{\beta 0y}y_c^2 + x'^2_c + y'^2_c
\end{aligned}
\tag{9}
$$

Use of eqs. (7) and (8) shows that:

$$
\frac{\mathrm{d}}{\mathrm{d}s}H = \frac{\mathrm{d}}{\mathrm{d}s} < h_{nl} > \tag{10}
$$

Thus if h_{nl} is not a function of s, H is an invariant.

Emittance Growth

We define separate x and y emittances: .

$$
\epsilon_x^2 \equiv 16(\Delta x^2 \Delta x'^2 - \Delta x x'^2); \qquad \epsilon_y^2 \equiv 16(\Delta y^2 \Delta y'^2 - \Delta y y'^2). \tag{11}
$$

Using eqs. (7), the following emittance evolution equations can be derived:

$$
\frac{\mathrm{d}}{\mathrm{d}s}\epsilon_x^2 = 32k^2_{\beta 0x}(\Delta x^2 \Delta x' x_m - \Delta x x' \Delta x x_m) + 32(\Delta(x\frac{\partial h_{nl}}{\partial x})\Delta x x' - \Delta x^2 \Delta(x'\frac{\partial h_{nl}}{\partial x})) \tag{12}
$$

$$
\frac{\mathrm{d}}{\mathrm{d}s}\epsilon_y^2 = 32(\Delta(y\frac{\partial h_{nl}}{\partial y})\Delta y y' - \Delta y^2 \Delta(y'\frac{\partial h_{nl}}{\partial y})) \tag{13}
$$

Thus the emittance would be constant if non-linearities were not present ($h_{nl} = 0$) and the momentum spread were absent ($x_m = 0$ for all particles.) Eqs. (12) and (13) are valid for both continuous and alternating gradient focusing.

Equilibrium Beam

In the continuous focusing approximation, the left-hand-sides of eqs. (7) and (8) can be set to zero to obtain the following equilibrium (constant moment) conditions:

$$\begin{aligned}
&\Delta x'^2 = (k_{\beta 0x}^2 - k_{sx}^2)\Delta x^2 - k_{\beta 0x}^2 \Delta x x_m + \Delta(x\tfrac{\partial h_{nl}}{\partial x}) \\
&\Delta y'^2 = (k_{\beta 0y}^2 - k_{sy}^2)\Delta y^2 + \Delta(y\tfrac{\partial h_{nl}}{\partial y}) \\
&\Delta x x_m = \tfrac{k_{\beta 0x}^2 \Delta x_m^2 - \Delta(x_m \frac{\partial h_{nL}}{\partial x})}{k_{\beta 0x}^2 - k_{sx}^2} \\
&x_c = < x_m > - \tfrac{1}{k_{\beta 0x}^2} < \tfrac{\partial h_{nl}}{\partial x} > \\
&y_c = -\tfrac{1}{k_{\beta 0y}^2} < \tfrac{\partial h_{nl}}{\partial y} > \\
&\Delta x x' = \Delta y y' = \Delta x' x_m = \Delta(x' \tfrac{\partial h_{nl}}{\partial x}) = \Delta(y' \tfrac{\partial h_{nl}}{\partial y}) = 0 \\
&x_c' = y_c' = 0
\end{aligned} \tag{14}$$

Assuming that $h_{nl} = x_c = y_c = 0$ the transverse energy (9) in equilibrium ($H = H_{eq}$) reduces to:

$$2H_{eq} = (2k_{\beta 0x}^2 - k_{sx}^2)\Delta x^2 + (2k_{\beta 0y}^2 - k_{sy}^2)\Delta y^2 - \frac{3k_{\beta x0}^4 \Delta x_m^2}{k_{\beta 0x}^2 - k_{sx}^2} - K\ln\left((\Delta x^2)^{1/2} + (\Delta y^2)^{1/2}\right) \tag{15}$$

Note that for a given H_{eq}, the ratio of Δx^2 to Δy^2 is still unspecified. A further assumption is required to specify the final state of the beam. It is often reasonable to assume that transverse energy equipartition results in a beam in which the two transverse temperatures are equal, i.e. $\Delta x'^2 = \Delta y'^2$. (Note that we have implicitly assumed that the timescale for complete equipartition $[\Delta x'^2 = \Delta y'^2 = \Delta(\delta p/p_0)^2]$ is much larger than timescales of interest.) The condition that $\Delta x'^2 = \Delta y'^2$ can be expressed as a relation between Δy^2 and Δx^2:

$$\Delta y^2 = \frac{(k_{\beta 0x}^2 - k_{sx}^2)}{(k_{\beta 0y}^2 - k_{sy}^2)}\Delta x^2 - \frac{k_{\beta 0x}^4}{(k_{\beta 0x}^2 - k_{sx}^2)}\Delta x_m^2 \tag{16}$$

When $k_{\beta 0x} = k_{\beta 0y} = k_{\beta 0}$ and $\Delta x_m^2 << \Delta x^2$ this result reduces to:

$$\Delta y^2 \cong \Delta x^2 - 2k_{\beta 0}^4 \Delta x_m^2 / \left(k^2(k^2 + k_{\beta 0}^2)\right), \tag{17}$$

where $k^2 \equiv k_{\beta 0}^2 - K/(4\Delta x^2)$.

Rings

Suppose a beam is in equilibrium in a straight section, and then enters a continuous bend (i.e. a ring). If the lattice parameters (such as the bend radius of curvature) abruptly change to new values, the beam becomes mismatched to the bend. Physically, particles that are not on the design momentum for the bend initially become spatially separated, creating non-linear space-charge forces, allowing phase mixing of the coherent mismatch oscillations until a new equilibrium is reached. For concreteness, we consider a lattice in which $k_{\beta 0x} = k_{\beta 0y} \equiv k_{\beta 0}$, and also assume that $k_{\beta 0}$ is the same both in the straight section and in the bend section. Thus, in this example, we assume the contribution to focusing from the bends is included in $k_{\beta 0}$. We assume that the initial beam (subscript 0) is matched to the straight section. Thus $\Delta y_0^2 = \Delta x_0^2$, and $\Delta x_0'^2 = \Delta y_0'^2 = k_0^2 \Delta x_0^2$, and all other moments are equal to zero. The initial transverse energy satisfies $2H_0 = (2k_{\beta 0}^2 + 2k^2)\Delta x_0^2 - K\ln[2(\Delta x_0^2)^{1/2}]$. To calculate the final equilibrium beam parameters, we set the final transverse energy equal to the initial transverse energy, and simultaneously solve this constraint with the equalized temperature constraint, eq. (16). Thus, there are two equations in two unknowns (Δx^2 and Δy^2), yielding the final equilibrium values of Δx^2 and Δy^2 in the bend. From the equilibrium values (eq. 14), all other second order moments may be calculated, including the emittance.

In ref. [3], comparisons of the results of the continuous focusing theory were made to 2D WARP PIC simulations of the transition from straight to bend for parameters of a small recirculator experiment being built at Lawrence Livermore National Laboratory. The relevant parameters of the simulation were: the ion species was singly charged Potassium, (mass 39), at an energy of 80 kV, and a current of 2 mA, leading to a perveance K of 3.54×10^{-4}. The average focusing constants are $k_{\beta 0x} = k_{\beta 0y} = 1.89\ \mathrm{m}^{-1}$, corresponding to a phase advance of 78 degrees and half-lattice period $L = 0.36$ m. The average bend radius of curvature is $\rho_0 = 2.29$ m. The normalized emittances $\epsilon_{nx} \equiv \gamma\beta\epsilon_x$ and $\epsilon_{ny} = \gamma\beta\epsilon_y$ (where γ is the Lorentz factor of the beam) were both set to 0.03 mm-mrad at injection into the ring. $\delta p/p_{0rms} = 7.2 \times 10^{-4}$ was assumed.

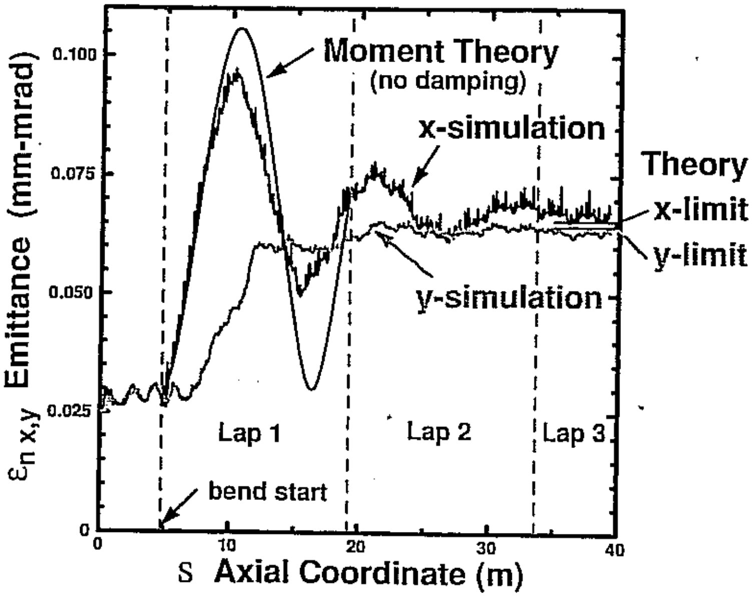

Figure 1. Comparison of WARP simulations with model results (from ref. [3]). x and y emittance evolution in a ring geometry, after initialization in a straight section, as calculated by WARP, by direct integration of the moment equations (Moment Theory, no damping) and the asymptotic value using energy conservation.

In Figure 1, (from ref. [3]), we plot the WARP simulations of the normalized x and y emittances over 3 laps of the small recirculator. In addition, we plot the initial evolution of the emittance as predicted by direct integration of the moment equations, (indicated as Moment Theory (no damping)) in the figure. The simulations include all of the details of alternating gradient lattice including fringe fields and image effects, as well as the non-linear space charge fields. The theory calculations use only the uniform focusing and bending approximation. Also, because the moment equations do not include non-linearities and the associated non-linear phase mixing, the amplitude of the x-emittance oscillations remain constant and the y-emittance does not grow. In the simulations, small non-linearities cause the oscillations to damp and the y-emittance to gradually grow closer to the x-emittance. Although direct integration of the moment equations does not capture the damping of the oscillations in the x-emittance or the growth in the y-emittance, the moment equations accurately predict the initial amplitude and frequency of the oscillations. Also shown on the figure are the final equilibrium results (indicated as x-limit theory, and y-limit theory) calculated using the prescription indicated above, which is based on using the moment equations to calculate the transverse energy and assuming equality of the final velocity spreads in the x and y directions. As can be seen, the theory closely predicts the asymptotic values of the x and y emittances as found by the fully 3D simulations, and also captures the simulation result that the y-emittance equilibrates to a value less than the x-emittance. Simulations of the University of Maryland Ring (ref. [15]) shows a similar increase in emittance with an ultimate saturation.

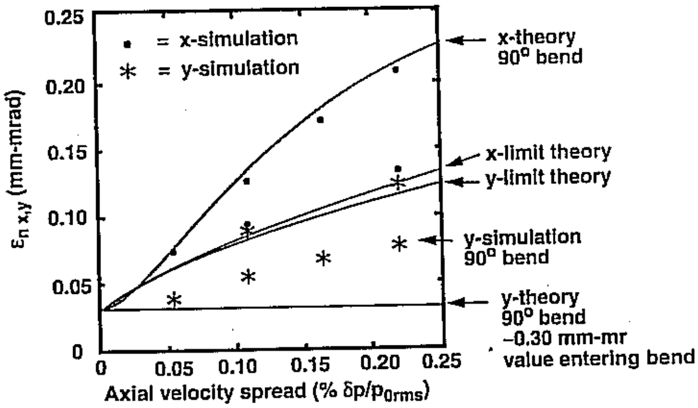

Figure 2. Comparison of WARP simulations with model results (from ref. [3]). x and y emittance after the 90 degree bend and asymptotic results as a function of the fractional momentum spread (in percentage), after initialization in a straight section, as calculated by WARP, by direct integration of the moment equations (x- and y- theory 90° bend) and the asymptotic value using energy conservation (x- and y- limit theory).

In Figure 2, (from ref. [3]), we plot the emittance at the end of ninety degrees of bend and also the asymptotic values of the emittance, all as a function of $\left(\Delta(\delta p/p_0)^2\right)^{1/2} \equiv \delta p/p_{0rms}$. This quantity is largely unknown in the experiment, and it could range anywhere from the value expected from accelerative cooling (see e.g. ref. [16]) of the longitudinal momentum spread induced by the ~0.1 eV ion source, which results in a spread of order 10^{-6}, or if the fractional error in the injector diode voltage errors is as large as 0.005 (at high enough frequency), the resulting induced fractional momentum spread, $\delta p/p_{0rms}$ would be as large as 2.5×10^{-3}. A third possible source of momentum spread comes from instabilities associated with an anisotropic velocity distribution (ref. [22]). If this instability heats the longitudinal component until it is of the same temperature as the transverse, the resulting moment spread would be $\delta p/p_{0rms} \cong \epsilon_x/4(\Delta x^2)^{1/2} \cong 7.2\times10^{-4}$. (For a more complete discussion cf. ref. [3]). As can be seen from the plot, direct integration of the moment equations closely captures the simulation value of the emittance after 90 degrees (during the initial emittance oscillation) and closely matches the mean rise in emittance and difference between the x and y emittances.

When $k_{\beta0x} = k_{\beta0y}$, and when the change in emittance is much less than the original emittance, one may analytically estimate the change in emittance squared in an abrupt transition from straight to bend:

$$\epsilon_x^2 - \epsilon_{x0}^2 \cong 16\frac{k_{\beta0}^4(2k_{\beta0}^2 + k^2)}{k^2(k_{\beta0}^2 + k^2)}\Delta x_0^2 \Delta x_m^2; \qquad \epsilon_y^2 - \epsilon_{y0}^2 \cong 16\frac{k_{\beta0}^6}{k^2(k_{\beta0}^2 + k^2)}\Delta x_0^2 \Delta x_m^2 \tag{18}$$

Eqs. (18) are valid only for small changes in emittance, and so are not applicable to the parameters of figure 1.

Racetracks

In a recirculator that is composed of two 180° bends connected by two straight sections in the shape of a racetrack, if phase mixing is rapid enough the equilibrium can be reached before each transition. Transverse energy is conserved as a beam enters a bend from a straight, but since the beam acquires a finite $\Delta x x_m$ as it finds equilibrium in the bend, the transverse energy will be discontinuous entering a straight from a bend, (where ρ_0 becomes infinite, and hence $\Delta x x_m$ abruptly changes to zero.) The quantities Δx^2, $\Delta x'^2$, Δy^2, $\Delta y'^2$ are, of course, continuous at all transitions. A new value of H is calculated which is again constant throughout the straight section. At the beginning of the bend the process repeats. In Fig. (3), we have applied this formulation to a small scale racetrack recirculator, which is not undergoing acceleration. This prescription for calculation of the emittance was carried out numerically, and compared with the 3-D version of the WARP code. As can be seen, the emittance growth is tracked closely although the higher frequency oscillatory behavior associated with lattice and mismatch oscillations are, of course, not seen. (For small values of $\Delta(\delta p/p_0)^2$, or large values of σ/σ_0 the prescription overestimates the emittance growth, since the assumption of complete phase-mixing between transitions is not achieved.)

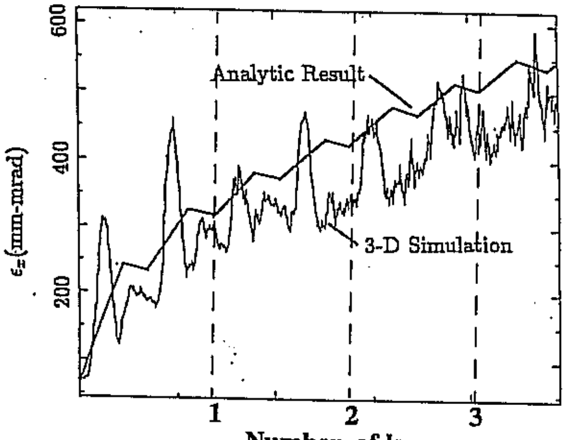

Figure 3. Emittance growth in a racetrack. The parameters are $\sigma_0 = 72°$, $\sigma = 8°$,

$\rho = 3.6\text{m}$, $Am_a\beta^2c^2/2 = 10\text{MeV}$, $(\Delta(\delta p/p_0)^2)^{1/2} = 0.0079$. The length of each straight section was 7.2 m.

Comparison to Other Recent Work

Recently, in ref. [4, 18], envelope equations which include the same physics (i.e. dispersion linear in $\delta p/p_0$, and space charge with an assumed elliptical symmetry) as the moment equations (eqs. 7,8) were derived. Venturini and Reiser found a generalized emittance ϵ_{dx} which, when expressed in terms of the notation of this paper can be written as:

$$\epsilon_{dx}^2 = (\Delta x_m^2 \Delta x^2 - \Delta x x_m^2)(\Delta x_m^2 \Delta x'^2 - \Delta x' x_m^2) - (\Delta x_m^2 \Delta x x' - \Delta x x_m \Delta x' x_m)^2 \tag{19}$$

By taking the derivative of ϵ_{dx}^2 and using eqs. (7), it is straightforward to show that ϵ_{dx}^2 is constant. By using the constancy of ϵ_{dx} and ϵ_y, two of the eight first order moment equations could be eliminated, leaving six first order moment equations, equivalent to the three second order equations of ref. [4]. Thus the envelope equations in ref. [4] contain the same physical content as the previously derived (ref. [1]) moment equations. In ref. [4], it is suggested that it would be possible to eliminate much of the growth in emittance by matching the envelope and the dispersion function $D(s) = (\Delta x \delta p/p_0)/\Delta(\delta p/p_0)^2$ (as defined in ref. [4]). This is equivalent to finding the matched periodic solution of the moment equations in the ring, and then constructing the section which injects the beam into the ring such that the values of the moments match those of the matched periodic solution within the ring. In order to prevent mismatch oscillations of the centroid, the centroid equations (8) must also be matched on the transition from straight to bend. Another method (ref. [1]) of preventing emittance growth is by slowly varying the radius of curvature, allowing an adiabatic transition into the bend.

Also, recently in ref. [5], vertical and horizontal dispersion functions are derived. The horizontal dispersion function derived by Lee is identical to that of ref. [4], except that horizontal/vertical coupling is allowed such as can occur if there are quadrupole rotation errors (see e.g. ref. [19]). The vertical dispersion function is identical to that of a straight lattice, but again with the inclusion of horizontal/vertical coupling. The envelope equations derived are not consistent with the moment eqs. (7,8) or the envelope equations of ref. [4], however, due to additional approximations.

Self-consistent distributions

Recently, in ref. [20], a self-consistent KV solution to the Vlassov-Poisson system in a bend was obtained. The solutions in the non-relativistic case are of the form:

$$f(x, x', y, y', \delta p/p_0) = f_\perp(H_\perp)\exp[-(\delta p/p_0)^2/\delta_0^2] \tag{20}$$

Here $2H_\perp = x'^2 + y'^2 + k_{\beta 0}^2 x^2 + k_{\beta 0}^2 y^2 + 2q\phi/mv_0^2 - 2(x/\rho_0)\delta p/p_0$. In ref. [20], generalizations to the KV distribution were investigated of the form $f_\perp(H_\perp) = f_0\delta(H_\perp - H_0)$. In ref. [21] thermal equilibrium distributions of the form $f_\perp(H_\perp) = f_0\exp(-H_\perp/k_bT)$ have been examined. Figure 4 illustrates the two distributions for the parameters of the University of Maryland electron ring experiment (ref. [20]) ($k_{\beta 0}^2 = 17.437$ m^{-2}, current = 105 mA, energy = 10 keV, $\rho_0 = 1.82$ m, with $k/k_{\beta 0} = 0.33$, and $\delta p/p_{0rms} = .01$.)

The moment eqs. require averages over xE_x and yE_y where E_x and E_y are the electric field components due to space charge. Although in ref. [1], an ellipse with uniform charge density was used to calculate E_x and E_y, as pointed out in ref. [7], the results also apply if the density is a function only of $x^2/\Delta x^2 +$

$y^2/\Delta y^2$, i.e. constant on nested elliptical surfaces (ref. [4]). As can be seen for the generalized KV distribution, the assumption of a density distribution that is constant on nested ellipses is poor for the KV distribution, but appears to be a better approximation for thermal equilibrium beams, which underlies the calculation of asymptotic emittance growth above. This may, in part, explain why the WARP simulation results agree well with the moment model.

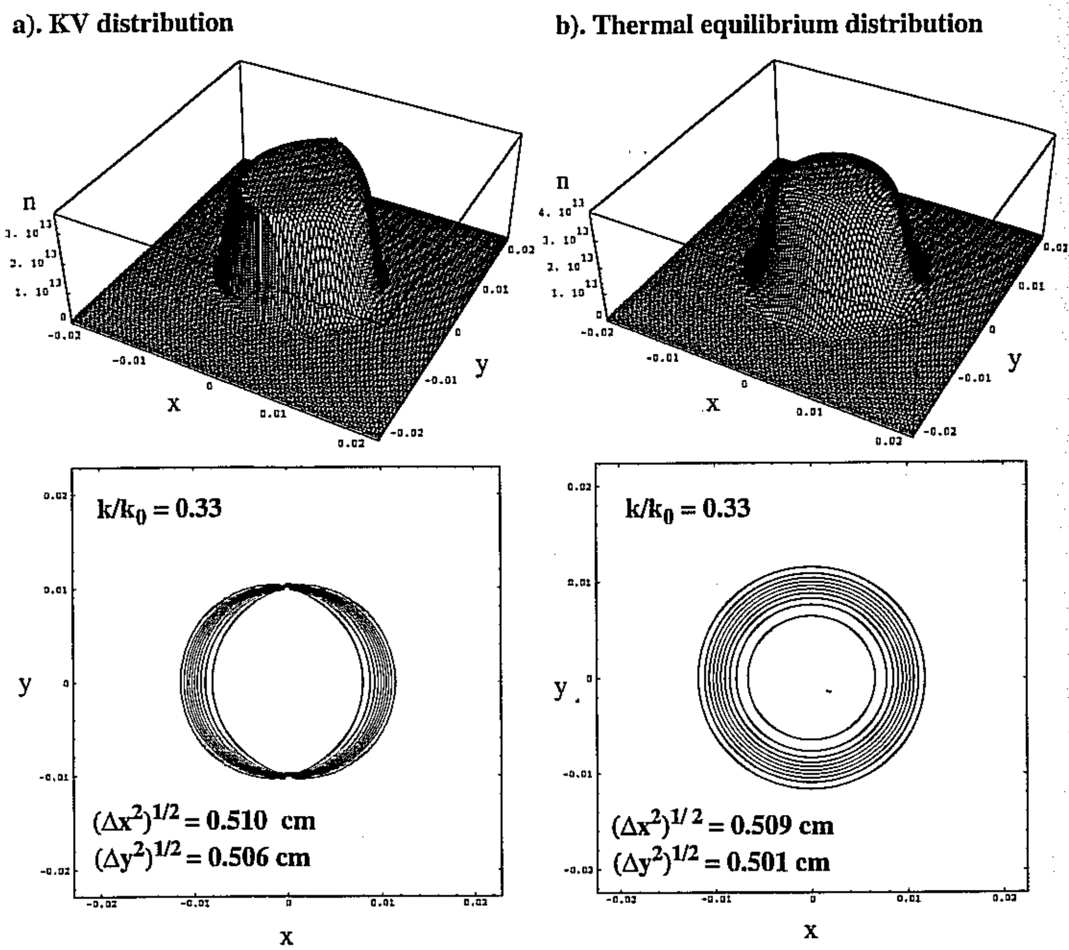

Figure 4. Self consistent beam density distributions in bends. a) Surface plot (upper) and contour plot (lower) of generalized KV distribution (ref. [20]); and b) Thermal distribution (ref. [21]).

Discussion

Emittance growth from sharp transitions, as discussed above, provides one source of emittance growth. Others, such as misalignments of quadrupoles, field strength errors, non-linear applied fields, etc., provide additional mechanisms to degrade the emittance. In the recirculator design of ref. [6], an insertion and extraction region occurs over a 100 m long straight section, which gives the machine some of the features of the racetrack in that equilibration can occur on passing from bend to straight and from straight to bend. Since the energy is increasing on each lap it would be difficult to design the insertion/ extraction section which is "matched" at all energies. Assuming abrupt transitions, use of the moment equations together with the parameters of the beam at the exit of the High Energy Ring of ref. [6] lead to an estimated emittance growth by a factor of about 2. Since the entrance beam parameters lead to a much smaller emittance growth, the normalized emittance will grow by less than a factor of 2. This is within the emittance "budget" in the design of ref. [6]. It is also possible that the transitions between bends and straights can be made gradual enough so that equilibria are reached adiabatically, with little associated growth in the normalized emittance.

Conclusions

We have reviewed the derivation of moment equations in which focusing, space charge, and dispersion in a bend, are included. We have shown that the moment equations derived in ref. [1], using the average bend and continuous focusing approximation, accurately predicts the initial amplitude and frequency of emittance oscillations which occur at a sharp transition from a straight section to a bend (ref. [3]). We have also reviewed the method of estimating the asymptotic value of the emittance growth due to straight/bend mismatches from considerations of transverse energy conservation as the beam equilibrates. By assuming the transverse energy of the beam is conserved during the equilibration, and assuming that the beam reaches equilibrium, and also that the equilibrium transverse velocity spread is the same in x as it is in y we can calculate all moments and thus the change in emittance. In racetracks, in which four such transitions are made per lap, we have calculated the emittance growth under the assumption that the equilibrium state is reached between each transition. In small scale rings the analytic result agreed well with 2-D and 3-D WARP simulations when σ/σ_0 was small and the velocity spread was sufficiently large (so that the assumption of phase mixing between transitions was realized). In the High Energy Ring of ref. [6], this prescription yielded an emittance growth of less than a factor of 2.

References

1. J.J. Barnard, H.D.Shay, S.S. Yu, A. Friedman, and D.P. Grote, "Emittance Growth in Heavy-Ion Recirculators,"1992 Linear Accelerator Conference Proceedings 1992 August 24-28, Ottawa, Ontario, Canada, C.R. Hoffman, ed. (1992). AECL 10728 (AECL Research, Chalk River, Canada) p. 229.
2. A. Friedman, D. P. Grote, D. A. Callahan, A. B. Langdon, I. Haber, "3D Particle Simulations of Axially Confined Heavy Ion Beams Using the WARP code: Transport Around Bends," Particle Accelerators, **37**, 131, (1992).
3. S.M. Lund, J.J. Barnard, G.D. Craig, A. Friedman, D.P. Grote, H.S. Hopkins, T.C. Sangster, W.M. Sharp, S. Eylon, T.J. Fessenden, E. Henestroza, S. Yu, and I. Haber, "Numerical Simulation of Intense-Beam Experiments at LLNL and LBNL," Nuclear Instruments and Methods A (in press).
4. Marco Venturini and Martin Reiser, "RMS Envelope Equations in the Presence of Space Charge and Dispersion," submitted to Phys. Rev. Letters (1998).
5. S.Y. Lee and H. Okamoto, "Space Charge Dominated Beams in Synchrotrons," these proceedings (1998).
6. J.J. Barnard, F. Deadrick, A. Friedman, D.P. Grote, L.V. Griffith, H.C. Kirbie, V.K. Neil, M.A. Newton, A.C. Paul, W.M. Sharp, H.D. Shay, R.O. Bangerter, A. Faltens, C.G. Fong, D.L. Judd, E.P. Lee, L.L. Reginato, S.S.

Yu, and T.F. Godlove, "Recirculating Induction Accelerators as Drivers for Heavy Ion Fusion," Physics of Fluids B: Plasma Physics, **5**, 2698 (1993). Also, "Study of Recirculating Induction Accelerators as Drivers for Heavy Ion Fusion," Lawrence Livermore National Laboratory UCRL-LR-108095 (1992).

7. F. J. Sacherer, "RMS Envelope Equations with Space Charge," IEEE Transactions on Nuclear Science **NS-18**, 1105, (1971).
8. P. M. Lapostolle, "Possible Emittance Increase through Filamentation Due to Space Charge in Continuous Beams," IEEE Transactions on Nuclear Science, **NS-18**, 1101, (1971).
9. T. P. Wangler, K. R. Crandall, R. S. Mills, and M. Reiser, "Relation Between Field Energy and RMS Emittance in Intense Particle Beams," IEEE Transactions on Nuclear Science, **NS-32**, (1985).
10. O. A. Anderson, "Internal Dynamics and Emittance Growth in Space-Charge-Dominated Beams," Particle Acclerators, **21**, 197, (1987).
11. J. J. Barnard, "Anharmonic Betatron Motion in Free Electron Lasers" Nuclear Instruments and Methods in Physics Research **A296** (1990).
12. M. Reiser "Free Energy and Emittance Growth in Nonstationary Charged Particle Beams," Journal of Applied Physics **70**, 1919 (1991).
13. O. A. Anderson, "Emittance Growth Rates for Displaced or Mismatched High Current Beams in Nonlinear Channels," Proc. of the Fourth NPB Techn. Symp., Argonne National Laboratory, (1992).
14. K. T. Nguyen "Emittance Growth and Energy Bandwidth in the IFRR," Proceedings of the 1990 DARPA/ SDIO/Services Annual Charged Part. Beam Review, p. 71, Nav. Res. Lab., Washington D. C. (1991).
15. R. A. Kishek, I. Haber, M. Venturini, and M. Reiser, "PIC Code Simulations of the Space-Charge-Dominated Beam in the University of Maryland Electron Ring," these proceedings.
16. M. Reiser, "Theory and Design of Charged Particle Beams," (Wiley & Sons, New York, 1994).
17. J.J. Barnard, J. Miller, I. Haber, "Emittance Growth in Displaced Space Charge Dominated Beams with Energy Spread," Proceedings of the 1993 Particle Accelerator Conference, Washington, D.C., May 1993, **5**, 3612. (1993)
18. M. Venturini, R.A. Kishek, and M. Reiser, "Dispersion and Space Charge," these proceedings (1998).
19. John J. Barnard, "Emittance Growth from Rotated Quadrupoles in Heavy Ion Accelerators," Proceedings of the 1995 Particle Accelerator Conference, Dallas TX, held May 1-5, 1995 (**5**), 3241 (1996).
20. M. Venturini and M. Reiser, "Self-consistent beam distributions with space charge and dispersion in a circular ring lattice," Phys. Rev. E, **57** 4725, (1998).
21. John J. Barnard, and Bojan Losic, "Emittance Growth from Bend/Straight transitions for Beams approaching Thermal Equilibrium," Proceedings of the 1998 Linear Accelerator Conference," In Preparation (1998).
22. I. Haber, D.A. Callahan, A. Friedman, D.P. Grote, S.M. Lund, T.F. Wang, "Characteristics of an Electrostatic Instability Driven by Transverse-Longitudinal Temperature Anisotropy", Nuclear Instruments and Methods A, in press (1998).